ISSN 1560-8034, 1605-6582 (On-line), SPQEO, 2019. V. 22, N 2. P. 156-164.

Semiconductor physics

Account of surface contribution to thermodynamic properties of lead selenide films

L.I. Nykyruy[1], B.P. Naidych[1], O.M. Voznyak[1], T.O. Parashchuk[2], R.V. Ilnytskyi[1]

[1]*Vasyl Stefanyk Precarpathian National University,*
57, Shevchenko Str., 76018 Ivano-Frankivsk, Ukraine,
E-mail: liubomyr.nykyrui@pu.if.ua, bvolochanska@i.ua
[2]*The Institute of Advanced Manufacturing Technology,*
Wrocławska 37, Krakow 30-011, Poland
E-mail: taras.parashchuk@ios.krakow.pl

Abstract. Being based on the density functional theory (DFT), computer simulation of the surface effect on thermodynamic parameters of lead selenide (PbSe) has been performed in this work. Applying the thermodynamic approach, the choice of model for the plane PbSe [200] preferred orientations has been justified, which indicates domination of the energy of surface states, while minimization of interface energy and deformation are less important in overall changing the free energy. The thermodynamic parameters for the surface of crystals and their temperature dependences in the framework of DFT method and using the hybrid functional B3LYP have been calculated, namely: energy ΔE, enthalpy ΔH, Gibbs' free energy ΔG, isobaric heat capacities C_P and isovolume heat capacities C_V, entropy ΔS. The analytical expressions of temperature dependences for these thermodynamic parameters approximated using quantum-chemical calculation data have been obtained. The analysis of temperature dependences for the heat capacity corresponds to the experimental data and the Djulong–Pti law.

https://doi.org/10.15407/spqeo22.02.156
PACS 05.70.Np, 68.35.Md, 71.15.Mb

Keywords: DFT, IV-VI semiconductors, cluster models, quantum-chemical calculations, thermodynamic properties.

Manuscript received 05.02.19; revised version received 24.04.19; accepted for publication 19.06.19; published online 27.06.19.

1. Introduction

The main advantage of lead chalcogenides (PbTe, PbSe, and PbS) is the small band gap (for example, 0.278 eV for PbSe at 300 K) [1]. This property is of great importance in infrared optics, lasers, light emitting devices, photovoltaics, and medium-temperature thermoelectric devices [2-5]. Therefore, in recent decades the purposeful work to find optimal conditions for their synthesis and application has been done. The areas of practical use of these compounds are not limited by the bulk samples. Applied devices were widely used based on thin films, quantum walls, supercells, nanowires, colloidal and embedded nanocrystals [6-9].

Application of PbSe in thermoelectricity is justified by a number of favorable characteristics. Namely, there are the low thermal conductivity at high temperatures [4], the minimum values of the band gap close to 0.3 eV at the L-point [10], the value of the Seebeck coefficient equal to (222.69 ± 0.02) μV/K and the possibility of its increase under deviation from stoichiometry in the direction to selenium [11], and the positive dependence of its changes with temperature [12]. The high thermoelectric efficiency is achieved for the combination of lead chalcogenides in ternary or quaternary solid solutions [8, 13-16].

At the modern stage of science and technology development, the lead selenide is used in thermo-electricity, optoelectronics and spintronic devices, especially in the long-wave range for production of infra-red diode lasers and thermo- or photoelectric energy converters [2, 17, 18]. An in-depth study of the properties of materials under different external conditions is associated with a wide spectrum of their application and sometimes of ambiguity observed in received results.

Simulation of the thermodynamic properties of crystals by using *ab initio* calculations is the least expensive in terms of material resources and duration of research. These methods have been popular for almost four decades and have proven themselves in enabling to

obtain the reliable information about properties of crystalline samples by using the minimum set of input data, to make their theoretical interpretation. On the other hand, the computer methods of quantum chemistry are the best for studying the nanoscale structures, which should be accompanied by the consideration of the near-order arrangement of atoms in real crystals, and by the analysis of its properties. The unconditional advantage of such approaches is convenience, accuracy and theoretical justification of research.

In this paper, based on *ab initio* calculations, using known crystallographic parameters, new approaches for determination of the main thermodynamic parameters of PbSe thin films and their temperature dependences have been proposed. And the experimental studies of isobaric heat capacity C_P have been carried out. The main attention is paid to the contribution of surface states to the values of thermodynamic parameters.

2. Computational details

Modern scientific and technological progress is dependent on the development of theoretical methods for researches. However, this success would have been impossible without the achievements of the novel computer approaches. First and foremost, they contribute to the improvement of model research. They are extremely convenient and satisfy the accuracy requirements for expanding and deepening information about the structure and properties of materials.

The value of the obtained results is greatly enhanced by the use of quantum-chemical methods for constructing the crystal structural models. The cluster approximation in the *ab initio* calculation is the most suitable and convenient method in this regard. The Avogadro software was used to simulate geometry of initial structures. All thermodynamical calculations for pristine PbSe have been performed using Firefly 8 package within Density Functional Theory (DFT) formalism [19].

Energy minimization was carried out through self-consistent field wave function using the Restricted Hartree–Fock (RHF) calculation. The convergence criteria for Self-Consistent Field (SCF) method calculations were chosen as $\Delta E_{SCF} = 10^{-4}$ eV. The calculations were carried out on the basis of Stevens–Basch–Krauss–Jasien–Cundari (SBKJC) parameterization [20]. DFT calculations were performed using hybrid DFT GGA with the Becke three-parameter hybrid method [21] with Lee, Yang, and Parr (B3LYP) gradient corrected correlation functional [22]. We did not use a supercell model, however a cluster approach was applied. The expediency of choosing this set has been proved in [23-25]. The Chemcraft software was used to visualize the results.

The PbSe compound crystallizes in a cubic granular structure of the type of NaCl (structural type B1) with the lattice parameter $a = 6.12$ Å [1, 18, 26], the spatial group is $Fm3m - O_h^5$. This position of atoms can be explained with account of lead chalcogenide relation to polar semiconductors characterized by the ionic-covalent type of bonds. The chosen structure allows the construction of clusters without involvement of additional atoms for the purpose to compensate the broken bonds. Crystal structures of lead sulfide have been investigated using four models, namely, on the base clusters with 64, 56, 27 and 8 atoms. Constructing the clusters, the main attention was paid to symmetry and electric charge of clusters to eliminate structural distortion caused by action of surface forces. This approach has been successfully used to creation of the cluster models for II-VI compounds [27, 28].

In IV-VI semiconductors, the valence electrons of lead form the sp^3-hybridized bonds with tellurium. Two *s*-electrons form deep narrow bands and practically do not take part in formation of bonding. Therefore, valence bands and conductive bands should be constructed from *p*-orbitals, which cubic symmetry reflects the cubic structure of bundles in IV-VI semiconductors. If the atoms of metal and chalcogen are chemically identical, then their fcc-lattice will turn into a simple cubic with an odd number of electrons (namely, three) in the cell. Therefore, under constructing the electronic spectrum of these compounds, it is necessary to include the Hamiltonian for the prophase of the ion potential, which describes the difference between metal atoms and chalcogen. This potential doubles the period of simple cubic lattice, and, as a result, even quantity of electrons ($3 \times 2 = 6$) is available in the new bcc-lattice, and the spectrum transforms to the dielectric type. By the order of magnitude, the potential of ion is close to the difference between the potentials of ionization of metal atoms and chalcogen [29].

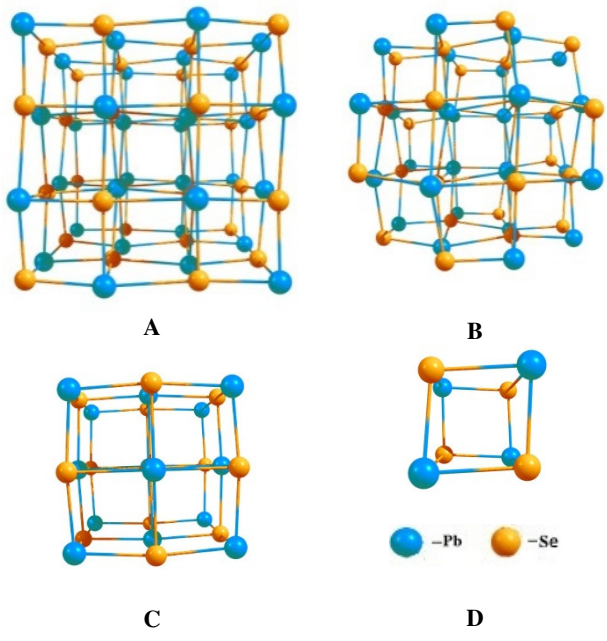

Fig. 1. Cluster models for cubic phase of PbSe: A ($Pb_{32}Se_{32}$), B ($Pb_{28}Se_{28}$), C ($Pb_{14}Se_{13}$), and D (Pb_4Se_4).

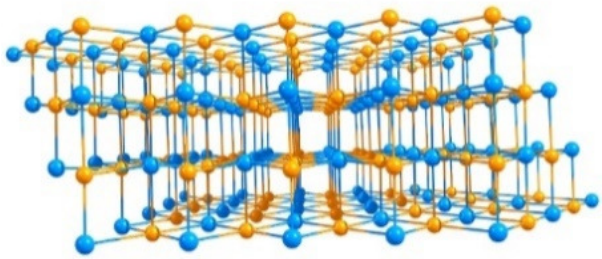

a)

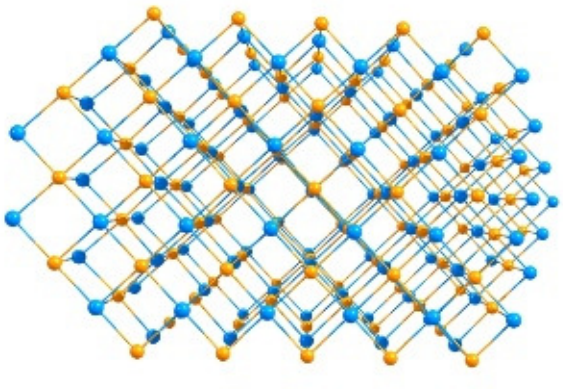

b)

Fig. 2. Models of PbSe films in the cross-section on (200) plane: front (a) and upper (b) images.

The first of the proposed cluster models (Fig. 1, A – the general formula is $Pb_{32}Se_{32}$) is the base for calculating both the spatial and electronic structure, as well as thermodynamic parameters. This model consists of 64 atoms and contains 4 pairs of six-coordinated atoms, 12 pairs of five-coordinated atoms, 12 pairs of four-coordinated atoms and 4 pair of three-coordinated atoms.

The second cluster has the general formula $Pb_{28}Se_{28}$ (Fig. 1, B) and consists of 56 atoms. It contains 4 pairs of six-coordinated atoms, 12 pairs of five-coordinated atoms, and 12 pairs of three-coordinated atoms.

The third cluster model contains 27 atoms and has the chemical formula $Pb_{14}Se_{13}$ (Fig. 1, C). This structure consists of one six-coordinated atom, 6 five-coordinated atoms, 12 four-coordinated atoms, and 8 three-coordinated atoms.

The fourth cluster with the formula Pb_4Se_4 (Fig. 1, D) is composed of 8 three-coordinated atoms.

At the first stage, the crystallographic parameters of the formed cluster were determined at the minimum potential energy and corresponded to the real position of the atoms in crystal. All the calculations began with SCF, next optimization of the geometry and the subsequent determination of stable minimum. Then, on the base of the obtained crystallographic parameters, the frequency of oscillations of atoms was calculated [30]. Visualization of spatial structures was carried out using Chemcraft software.

This approach enables to compile a system of equations for calculation of the thermodynamic values for selected clusters. As a result, we obtain the values of these parameters for three-, four-, five- and six-coordinated atoms, of which the cubic structure of NaCl forms itself.

Investigation of the films by using model approaches is based on assumption that real structures are limited in space, finite and not symmetrical along all directions.

Model images of the surface according to different projections are shown in Fig. 2. As our study has showed, this model corresponds to the experimental data. This choice is consistent with other researches and enables to simulate the effect of surface. In particular, the plane PbSe (200) is the preferred growth plane, when the surface energy minimization dominates in the total free energy variation [31].

3. Theoretical approach of thermodynamic calculations

3.1. Thermodynamic characteristics of crystals

In approximation of the fixed molecule [32], the enthalpy H of crystal formation is defined as:

$$H \approx H_{elec} + H_{vib}^{0} + E_{vib}(T) + H_{rot}(T) + H_{trans}(T) + RT, \quad (1)$$

where H_{elec} is the electronic component of enthalpy, H_{vib} – vibration component of enthalpy, H_{vib}^{0} – enthalpy of zero vibrations, H_{rot} – rotational component of enthalpy, H_{trans} – translational component of enthalpy, R – universal gas constant, T is absolute temperature in K. Similarly, the energy of formation was calculated.

In general, the entropy of the crystal is determined by the sum of components:

$$\Delta S = S_{trans} + S_{rot} + S_{vib} + S_{elec} - nR\left[\ln(nN_0) - 1\right], \quad (2)$$

where N_0 is the Avogadro constant, n is the number of the mole of molecules.

We can calculate the free Gibbs energy of the crystal at known temperature T by calculating the contributions of the energy of zero vibrations and of individual entropy parts of the reagent molecules A (Pb) and B (Te).

$$\Delta G = H_A - H_B + \frac{1}{2}\sum_{i\in A} h\nu_i - \frac{1}{2}\sum_{j\in B} h\nu_j - \\ - T\left(S_{vib}^{A} - S_{vib}^{B} + S_{rot}^{A} - S_{rot}^{B} + S_{trans}^{A} - S_{trans}^{B}\right). \quad (3)$$

To calculate ΔE, ΔH, ΔS, ΔG, C_V and C_P, used was the following method taking into account the initial conditions, on the example of formation energy ΔE. Initially, the energy of formation ΔE_A of the cluster A (Fig. 1, A) was calculated according to [32]:

$$\Delta E_A = E - \sum E_{el} + \sum E_{at}\,, \tag{4}$$

where E is the total energy of the system, E_{el} – electron energy of the atoms forming the system (in the atomic state), E_{at} – atomization energy. The total and electronic energies of the system were used from the calculation results, and all the other values were taken from references [33]. Similarly, the formation energies ΔE_B, ΔE_C and ΔE_D for clusters B, C and D (Fig. 1, B, C, D) were calculated.

The thermodynamic characteristics of PbSe crystals at different temperatures were calculated on the basis of computed vibrational spectra (Figs. 3 to 7).

As a result of quantum-chemical calculations, the values of each thermodynamic quantity for the corresponding clusters were obtained. Based on the consideration that these values were obtained as a set of these values for each individual atom in the cluster, each equation consists of the sum of contributions of all atoms, among which there are, respectively, three-, four-, five-, and six-coordinated atoms:

$$\begin{cases} 8x_3 + 24x_4 + 24x_5 + 8x_6 = A, \\ 24x_3 + 24x_5 + 8x_6 = B, \\ 8x_3 + 12x_4 + 6x_5 + x_6 = C, \\ 8x_3 = D, \end{cases} \tag{5}$$

where x_i (i = 3, 4, 5, 6) are the contributions of the corresponding three-, four-, five-, and six-coordinated atoms to the end value of thermodynamic parameters (in this case to the end value of formation energy ΔE_i), i is the number of atomic bonds formed. The factors before the values x_i denote the number of corresponding atoms in the cluster; ΔE_A, ΔE_B, ΔE_C, and ΔE_D – values of thermodynamic parameters (in this case, for formation energies under known temperature) for the corresponding clusters A, B, C, D (Fig. 1).

Having solved this system relatively to x_6, we obtain the following relation:

$$x_6 = \frac{A}{2} + \frac{5D - B}{4} - C\,. \tag{6}$$

Heat capacity at constant volume of C_V (similarly to C_P), in accordance with the given approximations is determined using the following formula:

$$C_V = S_{V(trans)} + S_{V(rot)} + S_{V(vib)}\,. \tag{7}$$

Contributions of translational degrees of freedom were calculated without data of quantum-chemical calculations, since they depend on external factors (T, P).

The contribution of the vibration component in the harmonic approximation, according to which the symmetry, relatively to the position of the displacement equilibrium, leads to symmetric change in the potential energy and is determined by the expression:

$$C_{V(vib)} = R\left(\frac{hc}{kT}\right)^2 \sum_i \frac{g_i \nu_i^2 e^{-\frac{hc\nu_i}{kT}}}{\left[1 - e^{-\frac{hc\nu_i}{kT}}\right]^2}\,. \tag{8}$$

where g_i is the degree of degeneracy of the i-th oscillation.

According to [34], the temperature dependence of the heat capacity of the crystalline structures is determined by the following function:

$$C = a + b \cdot 10^{-3} T - c \cdot 10^5 T^{-2}\,, \tag{9}$$

where a, b, c are the constant coefficients, which depend on the type of crystalline lattice and chemical compound.

3.2. Thermodynamic characteristics of the surface layers

Created on the surface of the crystal are the bonds directed inside the structure and along the surface. Thus, the surface layer of cubic crystal is formed by three-, four-, and five-coordinated atoms. To define the thermodynamic characteristics for these atoms, the same cluster models as for internal atoms can be used, but in this case the system (5) is solved with regard to x_3, x_4 and x_5. We obtained the following relations for these atoms:

$$x_3 = \frac{D}{3}\,, \tag{10}$$

$$x_4 = \frac{A - B}{24} + \frac{D}{12}\,, \tag{11}$$

$$x_5 = \frac{2C - 26D - A}{6} + \frac{B}{8}\,. \tag{12}$$

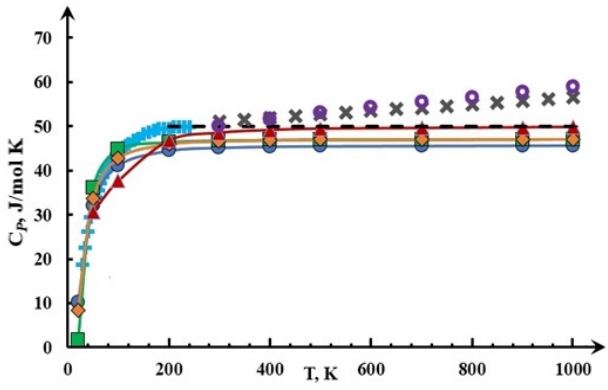

Fig. 3. Temperature dependences for the isobaric heat capacity of PbSe: ● – for three-coordinated atoms, ♦ – for four-coordinated atoms, and ■ – for five-coordinated atoms, ▲ – for six-coordinated atoms and comparing with experimental data: ○ – [40], × – [42], + – [36], -- – the theoretical curve according to the Djulong–Pti law.

Table 1. The coefficients of approximation of the temperature dependences of thermodynamic parameters: energy ΔE, enthalpy ΔH, Gibbs free energy ΔG, entropy ΔS, and isobaric heat capacity C_P.

Thermodynamic parameters	Approximation coefficients			The number of atomic bonds
	a_i	b_i	c_i	
The energy of formation, ΔE	0.016	58.742		6
	0.0105	104.66		5
	0.0173	102.36		4
	0.0097	104.76		3
Enthalpy, ΔH	0.0146	58.742		6
	0.0162	102.36		5
	0.0109	104.66		4
	0.0102	104.76		3
Entropy ΔS	20.497	54.11		6
	15.622	28.828		5
	9.2478	84.726		4
	8.4562	91.997		3
Gibbs free energy, ΔG	60.198	20.3	2	6
	6.046	1.6	2	5
	4.2496	22.3	1	4
	4.2099	25.8	1	3
Specific heat capacity, C_P	32.784	22.932	0.148	6
	45.777	1.784	0.179	5
	43.456	4.875	0.144	4
	41.945	4.956	0.131	3

Table 2. Experimental data and those calculated in this paper for thermodynamic parameters of PbSe semiconductor at the temperature 273.15 K.

	ΔH	ΔG	ΔS	C_p
Reference data	102.58 [35] 105.0 ± 4.0 [36] 106.7 ± 4.0 [37] 83 [41]	–(97.9 ± 7.7) [38] –101.577 ± 2.092 [39] –106.4 [40]	102.58 [36] 107.9 ± 4.0 [41] 102.51 ± 2.09 [39]	50.6 ± 1.0 [42] 51.14 [41] 50.21 [40]
Calculation data (in this paper, for six-coordinated atoms)	112.31	100.3	117.67	48.45

4. Results and discussion

The changes in the energy of formation ΔE, enthalpy of formation ΔH, Gibbs free energy ΔG, entropy ΔS, isovolume heat capacity C_V, and isobaric heat capacity C_P for PbSe crystals within the temperature range from 20 up to 1000 K are shown in Figs 3 to 7.

The temperature dependences of the thermodynamic parameters of lead selenide crystals within this temperature range after approximation by using the mathematical package Maple 18 yield the following dependences:

$$\Delta E(T) = a_i T + b_i, \quad (13)$$

$$\Delta H(T) = a_i T + b_i, \quad (14)$$

$$\Delta S(T) = a_i \ln(T) - b_i, \quad (15)$$

$$\Delta G(T) = a_i + b_i \cdot 10^{-3} T - c_i \cdot 10^{-5} T^2. \quad (16)$$

The calculated analytical expressions of the obtained temperature dependences for the isovolume and isobaric heat capacities, respectively, approximated using the quantum-chemical calculation points, are described by the following equations:

$$C_P = a_i + b_i \cdot 10^{-3} T - c_i \cdot 10^{5} T^{-2}. \quad (17)$$

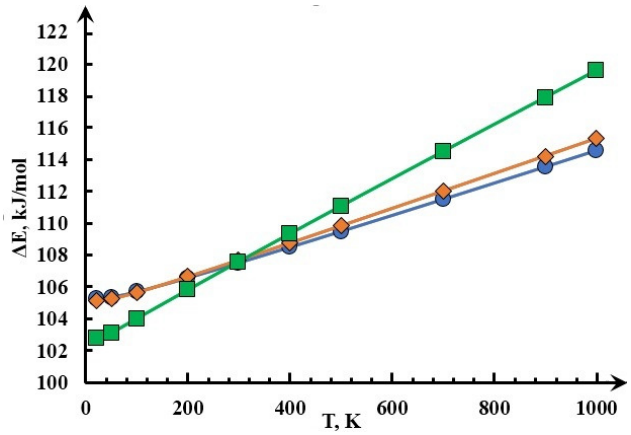

Fig. 4. Temperature dependences of energy (Δ*E*) for cubic PbSe crystals: ● – for three-coordinated atoms, ♦ – for four-coordinated atoms, ■ – for five-coordinated atoms.

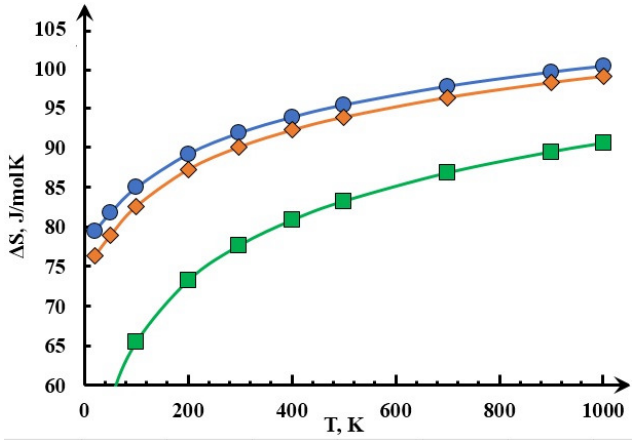

Fig. 5. The temperature dependences of the entropy (Δ*S*) for PbSe: ● – for three-coordinated atoms, ♦ – for four-coordinated atoms, ■ – for five-coordinated atoms.

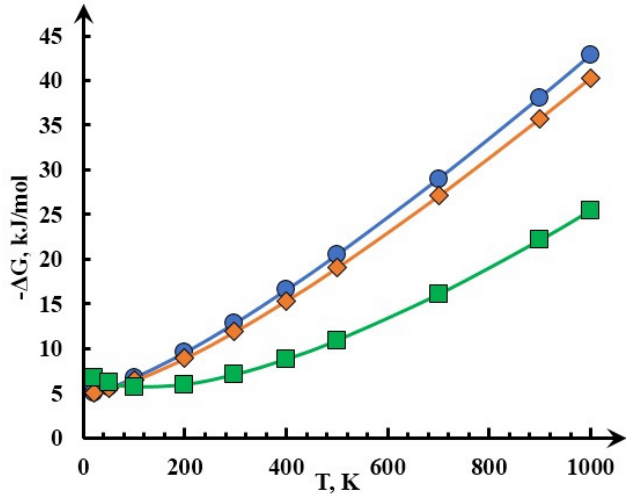

Fig. 6. Temperature dependences of Gibbs free energy (Δ*G*) for PbSe: ● – for three-coordinated atoms, ♦ – for four-coordinated atoms, ■ – for five-coordinated atoms.

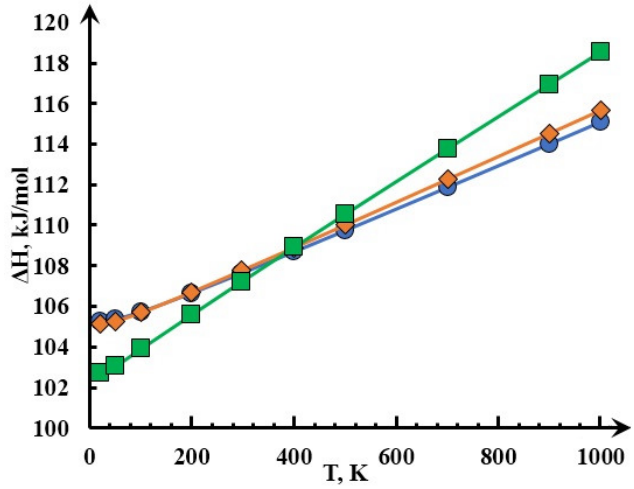

Fig. 7. Temperature dependences of the enthalpy (Δ*H*) for PbSe surface atoms: ● – for three-coordinated atoms, ♦ – for four-coordinated atoms, ■ – for five-coordinated atoms.

The obtained values of isovolume heat capacity C_V and isobaric heat capacity C_P at different temperatures are shown in Fig. 3. Good accordance with theoretical data can be reached by fitting the obtained calculation data to the classical law by Djulong and Pti. In the low temperature range, the obtained values are proportional to T_3, which corresponds to the Debye theory. Also, comparison of the calculation results with the measured experimental values was performed.

The slight deviations from the rectangular cross-position of the crystalline planes also were observed in the modelling of the PbSe structure in [43], using the GAUSSIAN 03 and SBKJC bases set. These results are confirmed by the experimental data in [44], as well as by the structural data in [45].

The deviation of the theoretically calculated equilibrium structure from the typical for rock salt lattice values can be explained by significant deviation of the lattice spectrum from the Debye spectrum [46]. Ionicity is the essential phase transition constraining factor. A similar effect is observed in spin-orbital interaction, since it violates the congruence of Fermi surface. This value for lead chalcogenides is large, which explains the lack of these transitions in respective compounds. However, the study of the phonon spectrum shows a strong softening of the optical phonon near the *G* point [47].

The changes of the formation energy Δ*E*, enthalpy Δ*H*, Gibbs free energy Δ*G*, the entropy Δ*S*, isovolume heat capacity C_V and isobaric heat capacity C_P for the surface of PbSe films within the temperature range 20…1000 K are shown in Figs. 3 to 7. Their analytical expressions have been represented as the dependences (13)–(17).

5. Conclusions

1. The cluster models and boundary conditions for calculation of thermodynamic parameters have been proposed as based on the crystalline and electronic structure of cubic PbSe, as well as its physical and chemical properties. It has been shown that the plane PbSe (200) is the preferred growth plane, when the surface energy minimization dominates over the total free energy variation.
2. The temperature dependences of thermodynamic parameters for PbSe crystals and films have been determined, namely: the energy of formation ΔE, enthalpy of formation ΔH, entropy ΔS and Gibbs free energy ΔG, as well as molar isovolume heat capacity C_V and isobaric heat capacity C_P.
3. Theoretical models of surface states of PbSe films have been proposed. The main thermodynamic parameters have been calculated on the base of this model. The obtained results are in good agreement with experimental data, in particular, for heat capacity at low temperatures [36]. For temperatures above 500 K, the monotonous growth of experimental values is observed, and the calculated values correspond to the law by Djulong and Pti.

References

1. Madelung O., Rössler U., Schulz M. (eds.) *Non-Tetrahedrally Bonded Elements and Binary Compounds I. Landolt-Börnstein – Group III Condensed Matter (Numerical Data and Functional Relationships in Science and Technology*), vol. 41C. Springer, Berlin, Heidelberg, 1988. https://doi.org/10.1007/10681727_890.
2. Eggleton B.J., Luther-Davies B., Richardson K. Chalcogenide photonics. *Nature photonics*. 2011. **5**, No 3. P. 141.
3. Khokhlov D. *Lead Chalcogenides: Physics and Applications*. CRC Press, 2002.
4. Dughaish Z.H. Lead telluride as a thermoelectric material for thermoelectric power generation. *Physica B: Condensed Matter*. 2002. **322**, No. 1–2. P. 205–223. https://doi.org/10.1016/S0921-4526(02)01187-0.
5. Haluschak M.O., Horichok I.V., Semko T.O. et al. Thermoelectric properties of solid solutions PbSnAgTe. *Physics and Chemistry of Solid State*. 2017. **18**, No 2. P. 211–214. https://doi.org/10.15330/pcss.18.2.211-214.
6. Kumar S., Khan Z.H., Khan M.M., Husain M. Studies on thin films of lead chalcogenides. *Current Applied Physics*. 2005. **5**, No 6. P. 561–566. https://doi.org/10.1016/j.cap.2004.07.001.
7. Fu H., Tsang S.W. Infrared colloidal lead chalcogenide nanocrystals: synthesis, properties, and photovoltaic applications. *Nanoscale*. 2012. **4**, No 7. P. 2187–2201. https://doi.org/10.1039/C2NR11836J.
8. Nykyruy L., Ruvinskiy M., Ivakin E., Kostyuk O., Horichok I., Kisialiou I., Yavorskyy Y. Hrubyak A. Low-dimensional systems on the base of PbSnAgTe (LATT) compounds for thermoelectric application. *Physica E: Low-dimensional Systems and Nanostructures*. 2019. **106**. P. 10–18. https://doi.org/10.1016/j.physe.2018.10.020.
9. Rogacheva E.I., Nashchekina O.N., Tavrina T.V., Us M., Dresselhaus M.S., Cronin S.B., Rabin O. Quantum size effects in IV–VI quantum wells. *Physica E: Low-dimensional Systems and Nanostructures*. 2003. **17**. P. 313–315. https://doi.org/10.1016/S1386-9477(02)00820-2.
10. Delin A., Ravindran P., Eriksson O., Wills J.M. Full-potential optical calculations of lead chalcogenides. *International Journal of Quantum Chemistry*. 1988. **69**. P. 349. https://doi.org/10.1002/(SICI)1097-461X(1998)69:3<349::AID-QUA13>3.0.CO;2-Y.
11. Vlasenko O.I., Levytsky S.M., Krys'kov Ts.A., Kyselyuk M.P. Thermoelectric properties of PbSe and PbS compounds. *Physics and Chemistry of Solid State*. 2006. **7**, No 4. P. 660.
12. Ravindra N.M., Srivastava V.K. Properties of PbS, PbSe, and PbTe. *phys. status solidi (a)*. 1980. **58**. P. 311. https://doi.org/10.1002/pssa.2210580139.
13. Snyder G.J., Toberer E.S. Complex thermoelectric materials. *Nature materials*. 2008. **7**. P. 105–114. https://doi.org/10.1038/nmat2090.
14. Horichok I.V., Nykyruy L.I., Galushchak M.O., Mudrij S.I., Semko T.O., Megilovska L.J., Gatala I.S., Yurchyshyn L.D. Synthesis and thermoelectric properties of PbTe-SnTe solid solutions. *Physics and Chemistry of Solid State*. 2016. **17**, No 4. P. 570–574. https://doi.org/10.15330/pcss.17.4.570-574.
15. Dow H.S., Oh M.W., Park S.D., Kim B.S., Min B.K., Lee H.W., Wee D.M. Thermoelectric properties of $AgPb_mSbTe_{m+2}$ $(12 \le m \le 26)$ at elevated temperature. *J. Appl. Phys*. 2009. **105**. P. 113703. https://doi.org/10.1063/1.3138803.
16. Horichok I., Ahiska R., Freik D., Nykyruy L., Mudry S., Matkivskiy O., Semko T. Phase content and thermoelectric properties of optimized thermoelectric structures based on the Ag-Pb-Sb-Te system. *J. Electron. Mater*. 2016. **45**. P. 1576–1583. https://doi.org/10.1007/s11664-015-4122-9.
17. Ren Y.X., Dai T.J., He B., Liu X.Z. Improvement on performances of graphene-PbSe Schottky photodetector via oxygen-sensitization of PbSe. *Mater. Lett*. 2019. **236**. P. 194–196. https://doi.org/10.1016/j.matlet.2018.10.045.
18. Virt I.S., Rudyi I.O., Lopatynskyi I.Ye., Dubov Yu., Tur Y., Lusakowska E., Luka G. *J. Electron. Mater*. 2017. **46**, No 1. P. 175. https://doi.org/10.1007/s11664-016-4903-9.
19. Granovsky Alex A., Firefly version 8, http://classic.chem.msu.su/gran/firefly/index.html.

20. Stevens W.J., Basch H., Krauss M. Compact effective potentials and efficient shared-exponent basis sets for the first- and second-row atoms. *J. Chem. Phys*. 1984. **81**. P. 6026. https://doi.org/10.1063/1.447604.
21. Becke A.D. A new mixing of Hartree–Fock and local density-functional theories. *J. Chem. Phys*. 1993. **98**, No 2. P. 1372. https://doi.org/10.1063/1.464304.
22. Lee C., Yang W., Parr R.G. Development of the Colle-Salvetti correlation-energy formula into a functional of the electron density. *Phys. Rev. B*. 1988. **37**, No 2. P. 785. https://doi.org/10.1103/PhysRevB.37.785.
23. Horichok I.V., Nykyruy L.I., Parashchuk T.O., Bardashevska D., Pylyponuk M.P. Thermodynamics of defect subsystem in zinc telluride crystals. *Modern Phys. Lett. B*. 2016. **30**, No 16. P. 1650172. https://doi.org/10.1142/S0217984916501724.
24. Naydych B. Calculation of the stability and rebuilding of the crystal surface within DFT-calculations. *Physics and Chemistry of Solid State*. 2018. **19**, No 3. P. 254–257. https://doi.org/10.15330/pcss.19.3.254-257.
25. Nykyruy L.I., Parashchuk T.O., Volochanska B.P. Thermodynamic parameters of lead sulfide crystals in the cubic phase. *Chalcogenide Lett*. 2016. **13**, No 6. P. 239.
26. Wang H., Pei Y., LaLonde A.D., Snyder G.J. Heavily doped *p*-type PbSe with high thermoelectric performance: An alternative for PbTe. *Adv. Mater.* 2011. **23**, P. 1366. https://doi.org/10.1002/adma.201004200.
27. Freik D., Parashchuk T., Volochanska B. Thermodynamic parameters of CdTe crystals in the cubic phase. *J. Crystal Growth*. **402**. P. 90. http://dx.doi.org/10.1016/j.jcrysgro.2014.05.005.
28. Freik D.M., Parashchuk T.O., Volochanska B.P., Duchenko I.V. Heat capacity and Debye temperature of CdTe, CdSe crystals. *Physics and Chemistry of Solid State*. 2014. **15**, No 2. P. 282.
29. Volkov B.A. Electronic properties of IV-VI narrow-band semiconductors. *Physics-Uspekhi*. 2003. **173**, No 9. P. 1013.
30. Yong D.C. *Computational Chemistry: A Practical Guide for Applying Techniques to Real-World Problems*. New-York: Wiley J.& Sons, Inc., 2001.
31. Sun X., Gao K., Pang X., Yang H. Interface and strain energy revolution texture map to predict structure and optical properties of sputtered PbSe thin films. *ACS Applied Materials & Interfaces*. 2015. **8**, No 1. P. 625–633. https://doi.org/10.1021/acsami.5b09724.
32. Chandrasekharan V., Walmsley S.H. The rigid molecule approximation in lattice dynamics. *Molecular Physics*. 1977. **33**, No. 2. P. 573. https://doi.org/10.1080/00268977700100491.
33. Haynes W.M. *CRC Handbook of Chemistry and Physics: A Ready-Reference Book of Chemical and Physical Data*. CRC Press, Boca Raton, Fla, 2010.
34. Tritt T.M. *Thermal Conductivity: Theory, Properties, and Applications*. Springer, Science & Business Media, 2005.
35. Stöber D., Hildmann B.O., Böttner H., Scheib S., Bachem K.H., Binnewies M. Chemical transport reactions during crystal growth of PbTe and PbSe via vapour phase influenced by AgI. *J. Crystal Growth*. 1992. **121**. P. 656–664. https://doi.org/10.1016/0022-0248(92)90572-Z.
36. Parkinson D.H., Quarrington J.E. The molar heats of lead sulphide, selenide and telluride in the temperature range 20 K to 260 K. *Proc. Phys. Soc., London, Sect. A*. 1954. **67**. P. 569–579. https://doi.org/10.1088/0370-1298/67/7/301.
37. Sadykov K.B., Semenkovich S.A. Study of the thermodynamic properties of lead selenide by the electromotive force method. *Izv. Akad. Nauk Turkmen. SSR, Ser. Fiz.-Tekh. Khim. Geol. Nauk*. 1966. **3**. P. 25–28 (in Russian).
38. Cox J.D., Wagman D.D., Medvedev V.A., *CODATA Key Values for Thermodynamics.* Hemisphere Publ. Corp., New York, 1989.
39. Robie R.A., Hemingway B.S., Fisher J.R. *Thermodynamic Properties of Minerals and Related Substances at 298.15 K and 1 Bar (105 Pascals) Pressure and at Higher Temperatures*. United States Government Printing Office, Washington, 1978.
40. Pashinkin A.S., Mikhailova M.S., Malkova A.S., Fedorov V.A. Heat capacity and thermodynamic properties of lead selenide and lead telluride. *Inorganic Materials*. 2009. **45**, No 11. P. 1226–1229. https://doi.org/10.1134/S0020168509110065.
41. Shamsuddin Misra S. Thermodynamic properties of lead selenide. *Scr. Metal*. 1973. **7**. P. 547–554. https://doi.org/ 10.1016/0036-9748(73)90110-5.
42. Blachnik R., Igel R. Thermodynamische Eigen-schaften von IV-VI-Verbindungen: Bleichalko-genide. *Z. Naturforsch*. 1974. **29b**. P. 625–629. https://doi.org/10.1515/znb-1974-9-1012.
43. Kiran B., Kandalam Anil K., Rallabandi R. et al. (PbS)32: A baby crystal. *J. Chem. Phys*. 2012. **136**. P. 024317. https://doi.org/10.1063/1.3672166.
44. Sun Q., Wang Y., Yuan X., Han J., Ma Q., Li F., Jin H., Liu Z. Preparation of PbS nano-microcrystals with different morphologies and their optical properties. *Cryst. Res. Technol.* 2013. **48**, No 9. P. 627. https://doi.org/10.1002/crat.201300189.
45. Littlewood P.B. Physics of Narrow Gap Semiconductors. *Proc. 4th Intern. Conf. on Physics of Narrow Gap Semiconductors*. Linz, Austria, 1981.
46. Toberer E.S., Zevalkink A., Snyder G.J. Phonon engineering through crystal chemistry. *J. Mater. Chem*. 2011. **21**, No 40. P. 15843–15852. https://doi.org/10.1039/C1JM11754H.
47. An J., Subedi A., Singh D.J. Ab initio phonon dispersions for PbTe. *Solid State Commun*. 2008. **148**, No 9–10. P. 417–419. https://doi.org/10.1016/j.ssc.2008.09.027.

Authors and CV

Lyubomyr Nykyruy, born in 1972, defended his Ph.D. in Physical and Mathematical Sciences in 2004. Docent (Ass. Prof.). Professor of Physics and Chemistry of Solids Department at the Vasyl Stefanyk Precarpathian National University. The area of his scientific interests includes the study of the features of transport phenomena in semiconductors; thermoelectric and photovoltaic properties of bulk, thin films and nanocrystalline semiconductor materials.

T.O. Parashchuk, born in 1989, defended Ph.D. in Physical and Mathematical Sciences in 2015. Postdoctoral Fellowship in the Institute of Advanced Manufacturing Technology, Krakow (Poland). The area of his scientific interests includes semiconductor materials for thermoelectricity, calculations of structural and electronic properties of semiconductors by using the DFT method.

B.P. Naidych, born in 1990, Ph.D. student, researcher. The area of her scientific interests includes technology of obtaining semiconductor materials, quantum-chemical calculations of thermodynamic properties of semiconductor crystals, temperature dependences of thermodynamic properties, temperature of phase transitions of binary semiconductor materials II-VI and IV-VI.

O.M. Voznyak, born in 1949, defended his PhD thesis in Physical and Mathematical Sciences in 1975. Docent (Ass. Prof.) of the Physics and Chemistry of Solids Department at the Vasyl Stefanyk Precarpathian National University. The area of his scientific interests includes theoretical studies concerning the properties of two-dimensional electron gas, spectrum of electronic excitations of disordered systems and their localization, study of transport phenomena in semiconductor materials with a narrow band gap by the variational method.

R.V. Ilnytskyi, born in 1977, defended his Dr. Sc. degree in 2017. Doctor of Physical and Mathematical Sciences, Professor, Head of Postgraduate and Doctoral Department at the Vasyl Stefanyk Precarpathian National University. The area of his scientific interests includes the methods for modifying the surface in materials for energetics, research of nano-dispersed titanium dioxide properties, *etc*.